W-Band ^{31}P-ENDOR on the High-Affinity Mn^{2+} Binding Site in the Minimal and Tertiary Stabilized Hammerhead Ribozymes

O. Schiemann[1], R. Carmieli[2], and D. Goldfarb[2]

[1] Institute of Physical and Theoretical Chemistry, J. W. Goethe University, Frankfurt, Germany
[2] Department of Chemical Physics, Weizmann Institute of Science, Rehovot, Israel

Abstract. The catalytic activity of the tertiary stabilized hammerhead ribozyme (tsHHRz) is by three orders of magnitude higher than the one of the long-known minimal construct (mHHRz). This gives rise to the question whether the single high-affinity manganese(II) binding site present in both ribozymes is located closer to the cleavage site and the transition state in the tsHHRz than in the mHHRz, which would make a direct involvement of this metal(II) ion in the bond-breaking step more likely. Here, we used W-band ^{31}P-Davies-ENDOR (electron–nuclear double resonance) to complement earlier reported ^{14}N-ESEEM/HYSCORE (electron spin echo envelope modulation/hyperfine sublevel correlation) studies. The ^{31}P-ENDOR spectrum of the mHHRz revealed a doublet with a splitting of 8.4($\pm$0.5) MHz but unresolved hyperfine anisotropy. Such a large splitting indicates an inner-sphere coordination of a phosphate backbone group with a significant amount of spin density on the phosphorous nucleus. This is in good agreement with the ^{31}P isotropic hyperfine constant, $A_{iso}(^{31}P)$, of +7.8 MHz obtained by density functional theory calculations on the structure of the Mn^{2+} binding site as found in crystals of the same ribozyme. This supports the idea that the structure and location of the binding site in the mHHRz is in frozen buffer similar to that found in the crystal. Since the W-band ENDOR spectrum of the tsHHRz also shows a ^{31}P splitting of 8.4($\pm$0.5) MHz, the local structures of both binding sites appear to be similar, which agrees with the coincidence of the ^{14}N data. An involvement of the high-affinity Mn^{2+} ion in the catalytic step seems therefore unlikely.

1 Introduction

Proteins are long known to be the machinery for catalysis and regulation within cells. In the 1980s this paradigm started to change due to the discovery of Thomas R. Cech [1] that some RNAs, so called ribozymes, can splice themselves in a catalytic fashion. Since then many additional functional roles of RNAs have been found [2], e.g., only RNA forms the peptidyl transferase center in the ribosome [3], interfering RNA (RNAi) is a natural antiviral mechanism of cells [4] and an RNA class called riboswitches regulates translation in bacteria [5].

Yet, the molecular mechanisms behind these biological functions are not fully understood. For the hammerhead ribozymes (small RNAs catalyzing the phosphodiester backbone cleavage reaction in the presence of divalent cations like Mg^{2+}) it is not even clear whether the divalent cations are directly involved in the cleavage step or if their sole purpose is to fold the RNA into the catalytic active conformation, whereas catalysis is performed by the neighboring bases [6]. Thus, methods which allow one to directly monitor metal(II) ions within the folded ribozyme are of high interest.

Substituting the naturally occurring diamagnetic Mg^{2+} by paramagnetic Mn^{2+} [7] permits to characterize the number of Mn^{2+} binding sites and their binding constants [8] and to study the local structure of the binding pocket [9]. Interestingly, the Mg^{2+}/Mn^{2+} substitution enhances the catalytic activity of hammerhead ribozymes up to 60-fold and does not lead to an inhibition [10].

Here, we investigate with W-band (95 GHz, ~3.4 T) ^{31}P-ENDOR (electron–nuclear double resonance) spectroscopy the binding of a single high-affinity Mn^{2+} ion to the RNA phosphate backbone of the minimal (mHHRz) [6] and tertiary stabilized hammerhead ribozyme (tsHHRz) [11] (Fig. 1). Both the catalytic activity [11] and the binding constant [12] of the tsHHRz are three orders of magnitude higher than those of the mHHRz, opening the question whether the high-affinity Mn^{2+} is located at the same site in both ribozymes or if the manganese(II) ion is bound closer to the cleavage site in the tsHHRz. On the basis of
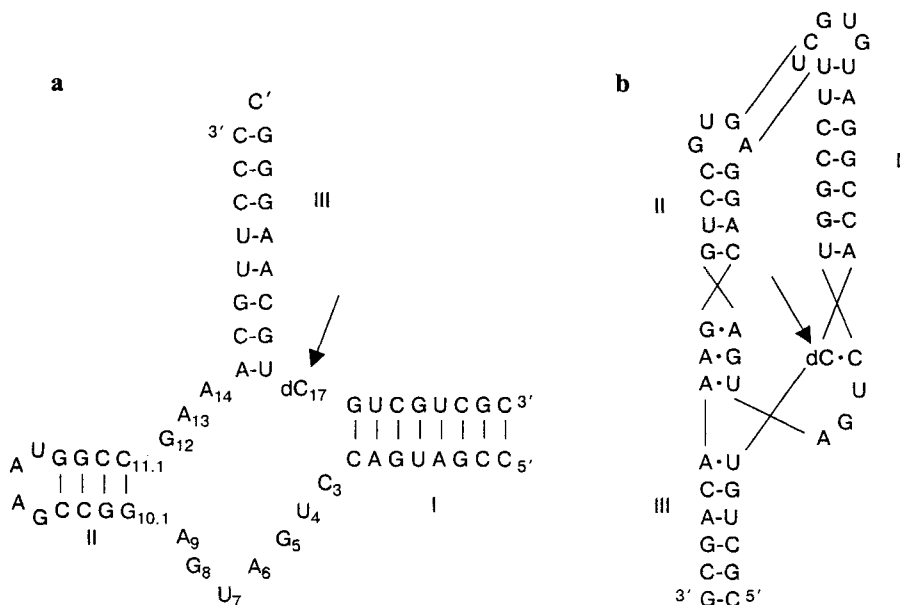

Fig. 1. Secondary structure of the mHHRz (a) and the tsHHRz (b). The arrows indicate the cleavage sites. The numbering of the stems follows the structural nomenclature.

crystal structures [13] and electron paramagnetic resonance (EPR) experiments in solution [9, 14], it is clear that the high-affinity Mn^{2+} in the mHHRz is bound to guanine G10.1 and the phosphate group between adenine A9 and G10.1, which positions the ion more than 1.5 nm away from the cleavage site. Therefore, this ion is most likely not directly involved in the catalytic step unless large structural rearrangements occur upon approaching the transition state. For the tsHHRz, the location and structure of the high-affinity Mn^{2+} binding site are uncertain. Scott et al. [15] published a crystal structure of the tsHHRz, but the ribozyme crystallized without divalent cations. Nevertheless, a comparative ^{14}N-ESEEM/HYSCORE (electron spin echo envelope modulation/hyperfine sublevel correlation) study of the m- and tsHHRz demonstrated that the high-affinity Mn^{2+} in the tsHHRz is bound to N7 of a guanine in a similar way as in the mHHRz [12], suggesting that both sites are structurally similar. In the study presented here we compare the binding of phosphate groups to the Mn^{2+} center in both ribozymes to complement the ^{14}N results.

2 Materials and Methods

2.1 Sample Preparation

The tobacco ringspot virus-derived ribozyme constructs used are depicted in Fig. 1. Both ribozymes were protected against cleavage by incorporation of a methoxy group at the 2′-sugar site of nucleotide C17 (denoted as dC in Fig. 1). All oligonucleotide strands were synthesized chemically by Dharmacon Research and received gel purified and desalted. High-performance liquid chromatography analysis showed that the strands were more than 95% pure. Autoclaved 0.1 M phosphate buffer solutions (pH 7.0) containing 1 M NaCl and 20% sucrose were added to yield final ribozyme concentrations of 0.4 mM for the pulsed EPR/ENDOR experiments. The manganese-phosphate buffer control sample had a concentration of 2 mM. Phosphate buffer was used to ensure correct folding and comparable data with respect to previous measurements. Sucrose was added to prevent clustering of the Mn^{2+}/ribozyme complexes upon freezing. The RNA concentrations were determined by UV-Vis using the extinction coefficients given in ref. 16. For annealing the ribozyme to the noncleavable substrate, the following temperature program was run: 90 °C for 3 min, 60 °C for 5 min, 50 °C for 5 min, 40 °C for 5 min and 22 °C for 15 min. A sterilized buffer solution of MnCl$_2$ (Sigma) was subsequently added to yield 1:0.9 ribozyme/Mn^{2+} complexes. Finally, the sample was heated again to 60 °C and cooled on ice to form the tertiary structure. For the pulsed EPR measurements, aliquots were loaded at room temperature into quartz capillaries (outer diameter, 0.84 mm, about 3 µl). Prior to the measurements, the probe head containing the sample was rapidly frozen by immersing it into liquid nitrogen and then transferred into the precooled cryostat.

2.2 EPR/ENDOR Measurements

W-band pulsed EPR/ENDOR measurements were carried out at 94.9 GHz and 6 K on a homebuilt spectrometer described elsewhere [17]. Field-sweep echo-detected EPR spectra were recorded using the two-pulse echo sequence ($\pi/2$-τ-π-τ-echo), where the echo intensity is monitored as a function of the magnetic field. Typically, microwave pulse lengths, t_{MW}, of 50 and 100 ns were used with $\tau = 0.4$ μs and 4 ms repetition time. The magnetic field values were calibrated against the proton Larmor frequency, ν_H, as determined by ^{1}H-ENDOR measurements (data not shown). Random acquisition was applied for all ENDOR measurements [18]. ^{31}P-ENDOR spectra were measured using the Davies-ENDOR pulse sequence (π-T-$\pi/2$-τ-π-τ-echo, with a radiofrequency (RF) π-pulse applied during the time interval T) with $t_{MW} = 0.2$, 0.1, 0.2 μs, respectively, and $\tau = 0.4$ μs. The RF pulse length, t_{RF}, was 25 μs for ^{31}P. The total number of accumulations per point was 6000 (30 shots, 200 scans).

3 Results

First, two-pulse echo-detected field-sweep EPR spectra were acquired at 94.9 GHz for the mHHRz/Mn^{2+} and tsHHRz/Mn^{2+} complexes both in 0.1 M phosphate buffer. A sample of Mn^{2+} in the same buffer without RNA was measured for the sake of comparison. It was taken care that the ribozyme-to-Mn^{2+} ratio was 1:0.9 to ensure the occupation of only the single high-affinity binding site in both ribozymes. All three samples displayed the typical Mn^{2+} EPR spectra with a sharp sextet on a broad background as illustrated for the mHHRz/Mn^{2+} complex in Fig. 2. The six lines centered around $g = 2$ belong to the hyperfine com-
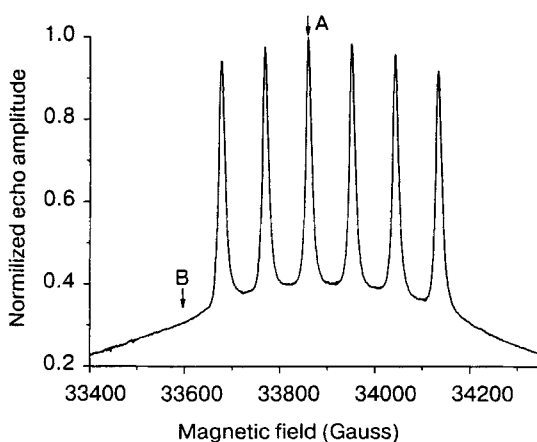

Fig. 2. Field-sweep echo-detected EPR spectrum of the Mn^{2+}/mHHRz complex. The two arrows A and B indicate the two field positions at which the ENDOR spectra where acquired.

ponents of the electronic $-1/2 \rightarrow +1/2$ transition of Mn²⁺ ($S = 5/2$, $I = 5/2$) with A_{iso}(Mn²⁺) amounting to 91 G. The broad background is due to the superposition of the powder patterns of all other electronic transitions.

Next, we performed W-band ³¹P-Davies-ENDOR measurements on the m- and tsHHRz samples to evaluate whether the Mn²⁺ is bound in both ribozymes to a RNA phosphate group, and if so, whether it is bound in the same way. The Mn²⁺/phosphate buffer sample was measured for the sake of comparison. Each ENDOR spectrum was acquired at field positions corresponding to the third line of the Mn²⁺ sextet (indicated by arrow A in Fig. 2) and they are presented in Fig. 3. All three ENDOR spectra are presumably due to the electronic $-1/2 \rightarrow +1/2$ transition, because application of the Davies-ENDOR pulse sequence on the broad background (arrow B in Fig. 2) instead of on the sextet does not show a ³¹P-ENDOR effect, most probably due to the low signal-to-noise ratio.

The ENDOR spectrum of the tsHHRz/Mn²⁺ complex, shown in Fig. 3b, exhibits a pair of broad lines split by about 8.4($\pm$0.5) MHz and centered around 58.4 MHz, the Larmor frequency of ³¹P at the magnetic field used, and is therefore assigned to ³¹P nuclei ($I = 1/2$) coupled to the Mn²⁺ ion. The anisotropy of the phosphorous hyperfine coupling is not resolved but covered under the large line width of 2.2($\pm$0.2) MHz measured as full width at half height. The large width of the peaks may either be due to heterogeneity within the site itself (e.g., A-strain) or to a structural heterogeneity of the ribozyme. The latter possibility mirrors itself in the fact that the tsHHRz reaches only a cleavage fraction of 60–80%, depending on the RNA sequence used [10, 19]. Thus, it might be that the tsHHRz predominantly folds into the catalytic active conformation (ca. 70%),
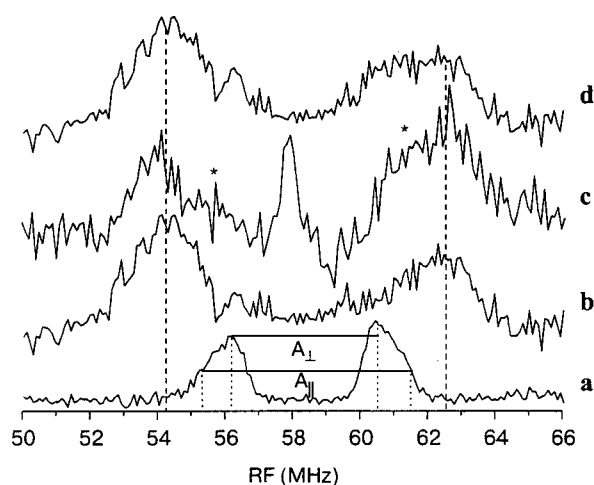

Fig. 3. W-band ³¹P-Davies-ENDOR spectra of Mn²⁺ in phosphate buffer (a), in the high-affinity binding site of the tsHHRz (b), in the high-affinity binding site of the mHHRz (c). d Sum of the spectra in a and b using a ratio of 1:3.5. The asterisks in c point to the shoulders due to Mn²⁺ free in solution.

but also into several inactive conformers. Such folding problems are commonly encountered with RNA [2].

In Fig. 3a, the ^{31}P-ENDOR spectrum of the control sample of Mn^{2+} in the phosphate buffer is shown. In contrast to the tsHHRz/Mn^{2+} sample, this one exhibits a splitting of about 4.3 MHz only, which is about half the splitting observed for the tsHHRz/Mn^{2+} sample, and a resolved hyperfine anisotropy. Reading off the frequencies at the turning points, indicated by dotted lines in Fig. 3a, yields $|A_\perp| = 4.3(1)$ MHz and $|A_{||}| = 6.3(1)$ MHz. An $A_{iso}(^{31}P)$ of 5 MHz and a $T_\perp \sim 0.7$ MHz are calculated using the following two equations and taking A_{iso} as positive:

$$A_\perp = A_{iso} - T_\perp,$$
$$A_{||} = A_{iso} + 2T_\perp.$$

This $T_\perp$ value yields a manganese–phosphorous distance of 0.36 nm using the point-dipole approximation:

$$|T_\perp| = \frac{g_e \cdot g_n \cdot \beta_e \cdot \beta_n}{h \cdot r^3}.$$

The distance as well as the magnitude of A_{iso} point to an inner-sphere coordination of the phosphate buffer ions. Comparing the ^{31}P-ENDOR spectra of the tsHHRz- (Fig. 3b) and of the Mn^{2+}/phosphate buffer proves that the spectrum of the tsHHRz is indeed due to Mn^{2+} bound to the tsHHRz and not to Mn^{2+} bound to the phosphate buffer.

The ^{31}P-ENDOR spectrum of the mHHRz/Mn^{2+} complex (Fig. 3c) reveals a ^{31}P-doublet separated by 8.4($\pm$0.5) MHz as for the tsHHRz, but in addition two shoulders at 55.4($\pm$0.3) and 61.4($\pm$0.3) MHz and a narrow peak at about the free Larmor frequency of [31]P. The shoulders are not assigned to a resolved hyperfine anisotropy, but to free Mn^{2+} ions bound to phosphate ions of the buffer. Indeed, a superposition of the tsHHRz/Mn^{2+} ENDOR spectrum with the spectrum of Mn^{2+} in phosphate buffer at a ratio of 3.5:1 yields the spectrum in Fig. 3d, which resembles the mHHRz/Mn^{2+} spectrum (phosphorus doublet with shoulders) nicely. The fact that RNA-unbound Mn^{2+} ions are only observed for the mHHRz can be related to the different dissociation constants of 4 µM [8] and <10 nM [12] for the m- and tsHHRz, respectively [20].

The occurrence of a peak at roughly the free Larmor frequency of ^{31}P in the mHHRz sample indicates the presence of distant, weakly coupled ^{31}P nuclei. These are, however, not due to free Mn^{2+} ions in the phosphate buffer since this peak does not appear in the Mn^{2+}/buffer spectrum. It is interesting to note that this peak neither showed up in the tsHHRz sample, suggesting that these ^{31}P nuclei interactions are characteristic for the mHHRz and may either be assigned to its phosphate backbone or to phosphate ions of the buffer bound closely to the binding pocket. This difference in the spectra of the m- and tsHHRz may be rationalized by comparing the two crystal structures, which show that the fold

of the tsHHRz is much more rigid and compact than the fold of the mHHRz [13, 15]. Therefore, the extended surrounding of both binding sites is clearly different and thus allows distant phosphate groups of the backbone to be close by in the m- but not in the tsHHRz. The other possibility could be that the more open conformation of the mHHRz permits phosphate ions of the buffer to bind close to the manganese binding pocket, whereas the compact fold of the tsHHRz could prevent this.

4 Discussion

The ^{31}P-Davies-ENDOR spectra of both ribozymes show a splitting of about 8.4 MHz and a broad line width of about 2.2 MHz, but no resolved hyperfine anisotropy. The splitting is larger than observed for other biological Mn^{2+}-phosphate complexes but resembles isotropic hyperfine coupling constants $A_{iso}(^{31}P)$ observed for manganese(II) aluminophosphates (Table 1). Such a large splitting can be explained by a large isotropic ^{31}P hyperfine coupling of about 8.4 MHz but not by a large hyperfine anisotropy. Even in an inner-sphere bound fashion, the manganese–phosphorus distance cannot be much closer than 0.34 nm, which would correspond to a $|T_\perp|$ of only 0.8 MHz as also found for the P_β of the Mn$^{2+} \cdot$ ADP [22] and the human p21ras $\cdot$ Mn$^{2+} \cdot$ GDP [25] complexes. On the other hand, assuming such an inner-sphere coordination results in a dipolar tensor width of $|T_\perp| \cdot 3/2 = 1.2$ MHz, which lies within the observed line width of about 2.2 MHz and agrees with the $|A_{iso}(^{31}P)|$ of about 8.4 MHz. In fact, such a large isotropic hyperfine coupling constant matches the $A_{iso}(^{31}P)$ of $+7.8$ MHz calculated by density functional theory (DFT) methods for the high-affinity binding site in the mHHRz [14]. The DFT calculations were based on the structure of the binding

Table 1. Isotropic ^{31}P hyperfine coupling constants for Mn^{2+}-phosphate complexes.

Complex[a]	$|A_{iso}(^{31}P)|$ (MHz)	Reference
Mn^{2+} in aqueous phosphate buffer (W-band Davies ENDOR)	~5	this work
MnAlPO$_4$-20	~8	21
Mn$^{2+} \cdot$ ADP (X-band HYSCORE)	4.5	22
Mn$^{2+} \cdot$ ATP (X-band HYSCORE)	4.5	22
Mn$^{2+} \cdot$ ATP (cw Q-band ENDOR)	P_β 4.0	23
Mn$^{2+} \cdot$ GMP (X-band Mims ENDOR)	0.08	24
Human p21ras$\cdot$Mn$^{2+} \cdot$ GDP (W-band Mims and Davies ENDOR)	P_α 0.02/P_β 4.7	25
Nitrogenase FeMo-protein Kp2$\cdot$Mn$^{2+} \cdot$ ADP (X-band HYSCORE)	4.4	26
Nitrogenase FeMo-protein Kp2$\cdot$Mn$^{2+} \cdot$ ATP (X-band HYSCORE)	5.4	26
mHHRz/Mn^{2+} (cw Q-band ENDOR)	~4	23
mHHRz/Mn^{2+} (DFT)	7.8	14
mHHRz/Mn^{2+} (W-band Davies ENDOR)	~8.4	this work
tsHHRz/Mn^{2+} (W-band Davies ENDOR)	~8.4	this work

[a] The method used to determine the magnitude of $A_{iso}(^{31}P)$ is given in brackets.

pocket as found in the crystal structure where one phosphate group is inner-
sphere bound at a manganese–phosphorus distance of 0.377 nm (Fig. 4). This
manganese-phosphorus distance yields a $|T_\perp|$ of 0.6 MHz and a tensor width of
0.9 MHz, which lies well within the line width. Interestingly, only structural ar-
rangements such as in the crystal structure lead to large $A_{iso}(^{31}P)$, whereas calcu-
lations on other structural arrangements or adenine instead of guanine produced
smaller values as those found for the biological manganese(II)-phosphate com-
plexes given in Table 1. (The DFT calculations will be reported in due course.)
Thus, not only the previously reported ^{14}N-HYSCORE/ESEEM [9, 14] but now
also the ^{31}P-ENDOR data agree well with the values calculated for the manga-
nese binding site in crystals of the mHHRz, emphasizing the previously drawn
conclusion that the structure and location of the high-affinity binding site in the
mHHRz is similar in frozen buffer and in the crystal.

Furthermore, the ^{31}P splitting is the same for the m- and tsHHRz indicating
a similar inner-sphere Mn^{2+}-phosphate coordination in both ribozymes, which is
again supported by the coincidence of the ^{14}N hyperfine and quadrupole data
found for both ribozymes [12]. Therefore, the local structure of the high-affinity
binding site seems to be comparable in both ribozymes. However, the low sig-
nal-to-noise ratio of the ^{31}P-ENDOR spectra prevents a definite answer to this
question. It also inhibits the analysis of line intensities in order to count the
number of coordinated phosphate groups [27] or to determine the absolute sign
of the hyperfine coupling constants [28]. Nevertheless, these W-band ^{31}P-Davies-
ENDOR measurements are the first to show the strongly coupled inner-sphere
bound phosphate group predicted by DFT calculations. Earlier cw Q-band ENDOR
studies on the mHHRz revealed only a splitting of about 4 MHz [23]. The reason
for the discrepancy with the data presented here is not clear but might be explained
by the ratio of specific and unspecific manganese to RNA binding. DeRose et al.
[24] also published X-band ^{31}P-ENDOR spectra but only for manganese(II) ions
bound to nucleosides, nucleotides or yeast tRNA^{Phe} which all reveal only small
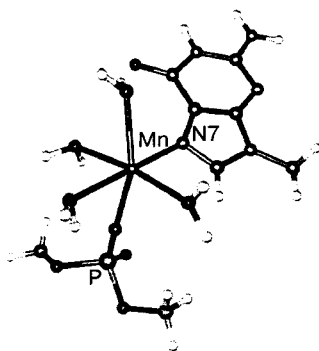^{31}P splittings.

Fig. 4. Local structure of the high-affinity manganese binding site as found in the crystal of the
mHHRz [13] and as used for the DFT calculations.

5 Conclusion

The W-band Davies-ENDOR spectra showed that the high-affinity Mn^{2+} ion is bound to a phosphate backbone group in both ribozymes. Furthermore, the large ^{31}P splitting observed for both ribozymes points to an inner-sphere manganese-phosphate binding with a significant amount of spin density on the phosphorous nucleus, $|A_{iso}| = 8.4(\pm 0.5)$ MHz. Such a large isotropic hyperfine coupling is in agreement with DFT calculations based on the mHHRz crystal structure, which predicted an A_{iso} of $+7.8$ MHz. Since the ^{14}N hyperfine and quadrupole data are also the same for both ribozymes, the local structure of the high-affinity binding site seems to be the same in both ribozymes. However, to answer the question if also the location of the site is the same in both RNAs, additional experiments are necessary as, for example, site-selective ^{15}N labeling of G10.1 in the tsHHRz and/or PELDOR measurements in combination with site-directed spin labeling to localize the manganese ion within the fold of the ribozyme.

Acknowledgments

References

1. Eckstein F., Lilley D.M. (eds.): Catalytic RNA. Nucleic Acids and Molecular Biology, vol. 10. Berlin: Springer 1997.
2. Gesteland R.F., Cech T.R., Atkins J.F. (eds.): The RNA World, 3rd edn. Cold Spring Harbor: Cold Spring Harbor Laboratory Press 2006.
3. Ban N., Nissen P., Hansen J., Moore P.B., Steitz T.A.: Science 289, 905–930 (2000)
4. Denli A.M., Hannon G.J.: Trends Biochem. Sci. 28, 196–201 (2003); Voinnet O.: Trends Genet. 17, 449–459 (2001)
5. Winkler W.C., Breaker R.R.: ChemBioChem. 4, 1024–1032 (2003)
6. Hammann C., Lilley D.M.: ChemBioChem. 3, 691–700 (2002)
7. Feig A.L. in: Manganese and Its Role in Biological Processes. Metal Ions in Biological Systems, vol. 37 (Sigel A., Sigel H., eds.), chap. 6. New York: Marcel Dekker 2000.
8. Horton T.E., Clardy D.R., DeRose V.J.: Biochemistry 37, 18094–18101 (1998)
9. Morrissey S.R., Horton T.E., Grant C.V., Hoogstraten C.G., Britt R.D., DeRose V.J.: J. Am. Chem. Soc. 121, 9215–9218 (1999)
10. Kisseleva N., Khvorova A., Westhof E., Schiemann O., Wolfson A.: RNA, in press (2006)
11. Khvorova A., Lescoute A., Westhof E., Jayasena S.D.: Nat. Struct. Biol. 10, 708–712 (2003)
12. Kisseleva N., Khvorova A., Westhof E., Schiemann O.: RNA 11, 1–6 (2005)
13. Pley H.W., Flaherty K.M., MacKay D.B.: Nature 372, 68–74 (1994); Scott W.G., Murray J.B., Arnold J.R.P., Stoddard B.L., Klug A.: Science 274, 2065–2069 (1996)
14. Schiemann O., Fritscher J., Kisseleva N., Sigurdsson S.T., Prisner T.F.: ChemBioChem. 4, 1057–1065 (2003)
15. Martick M., Scott W.G.: Cell 126, 309–320 (2006)
16. Gray D.M., Hung S.H., Johnson K.H.: Methods Enzymol. 246, 19–34 (1995)
17. Gromov I., Krymov V., Manikandan P., Arieli D., Goldfarb D.: J. Magn. Reson. 139, 8–17 (1999)

18. Epel B., Arieli D., Baute D., Goldfarb D.: J. Magn. Reson. **164**, 78–83 (2003)
19. Osborne E.M., Schaak J.E., DeRose V.J.: RNA **11**, 187–196 (2005)
20. Klotz I.M.: Ligand Receptor Energetics. A Guide for the Perplexed. New York: Wiley-Interscience Publication 1997.
21. Arieli D., Delabie A., Vaughan D.E.W., Strohmaier K.G., Goldfarb D.: J. Phys. Chem. B **106**, 7509–7519 (2002)
22. Schneider B., Sigalat C., Amano T., Zimmermann J.-L.: Biochemistry **39**, 15500–15512 (2000)
23. Morrissey S.R., Horton T.E., DeRose V.J.: J. Am. Chem. Soc. **122**, 3473–3481 (2000)
24. Hoogstraten C.G., Grant C.V., Horton T.E., DeRose V.J., Britt R.D.: J. Am. Chem. Soc. **124**, 834–842 (2002)
25. Bennati M., Hertel M.M., Fritscher J., Prisner T.F., Weiden N., Hofweber R., Spörner M., Horn G., Kalbitzer H.R.: Biochemistry **45**, 42–50 (2006)
26. Petersen J., Gessner C., Fisher K., Mitchel C.J., Lowe D.J., Lubitz W.: Biochem. J. **391**, 527–539 (2005)
27. Potapov A., Goldfarb D.: Appl. Magn. Reson. **30**, 461–477 (2006)
28. Manikandan P., Carmieli R., Shane T., Kalb A.J., Goldfarb D.: J. Am. Chem. Soc. **122**, 3488–3494 (2000)

Authors' address: Olav Schiemann, Institute of Physical and Theoretical Chemistry, J. W. Goethe University, Max-von-Laue-Strasse 7, 60438 Frankfurt, Germany
E-mail: o.schiemann@prisner.de